Моделирование процессов терлообмена в воздушном потоке, несущем капли над взволнованной водной поверхностью

О.А. Дружинин
Институт прикладной ф изики РАН, Нижний Новгород

Data on droplets generation by the wind (Andreas et al. 2010, JGR)

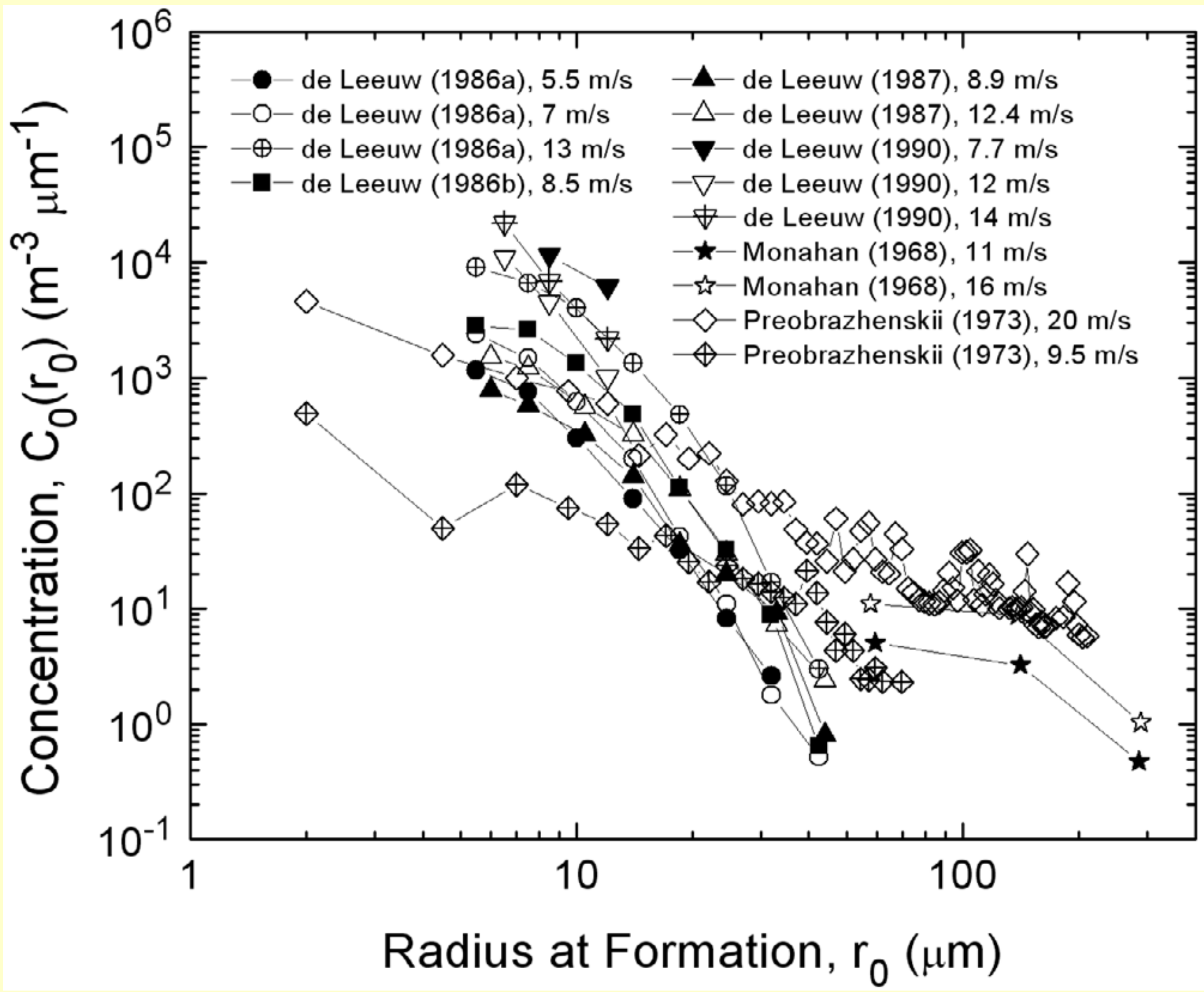

Droplet number density at different wind speeds at heights from 1 to 2m.

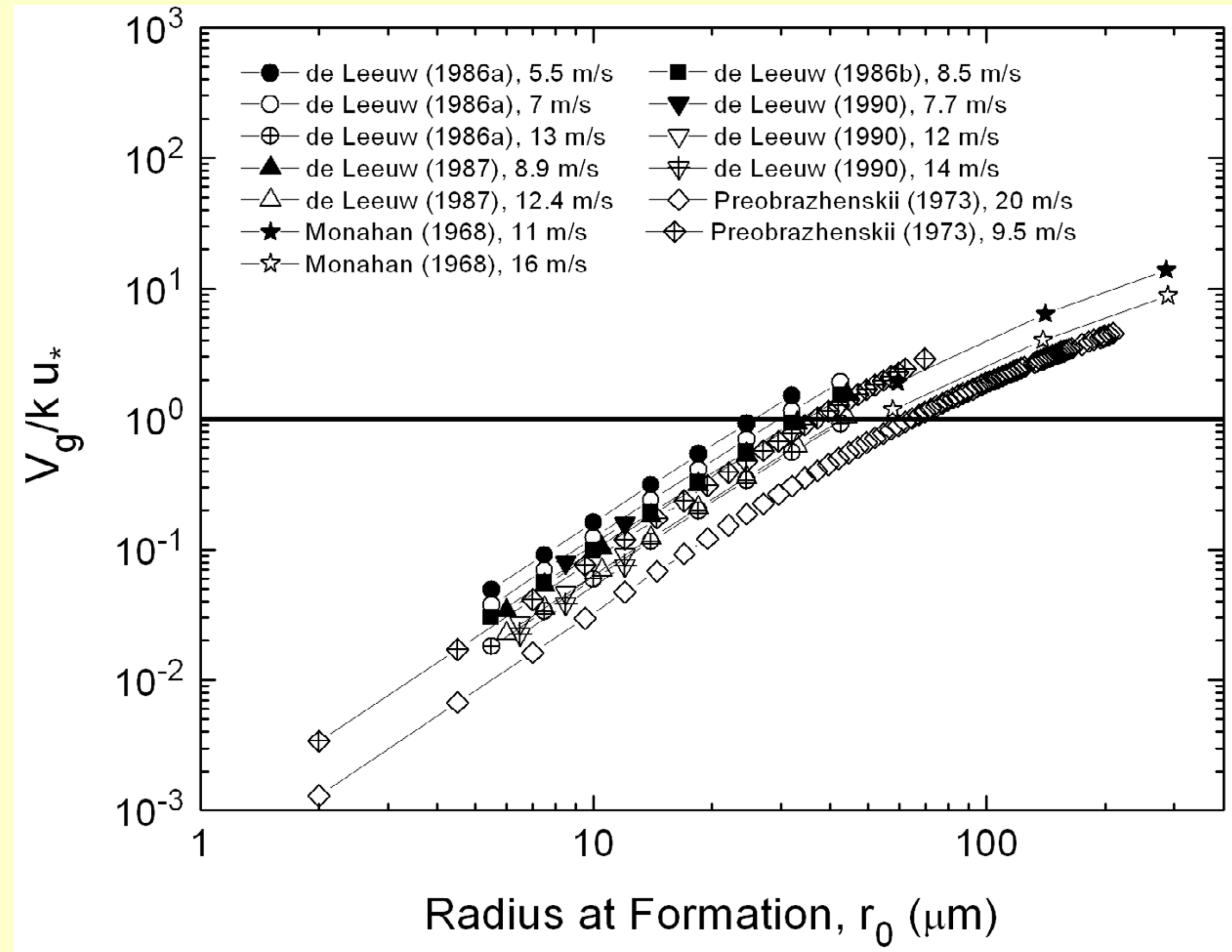

Droplet terminal velocity normalized by friction velocity and Karman constant (k=0.4)

$$\left(V_g = g\frac{d^2}{18\nu}\frac{\rho_w}{\rho_a} \right)$$

Lab experiments

Komori at al. 2018)

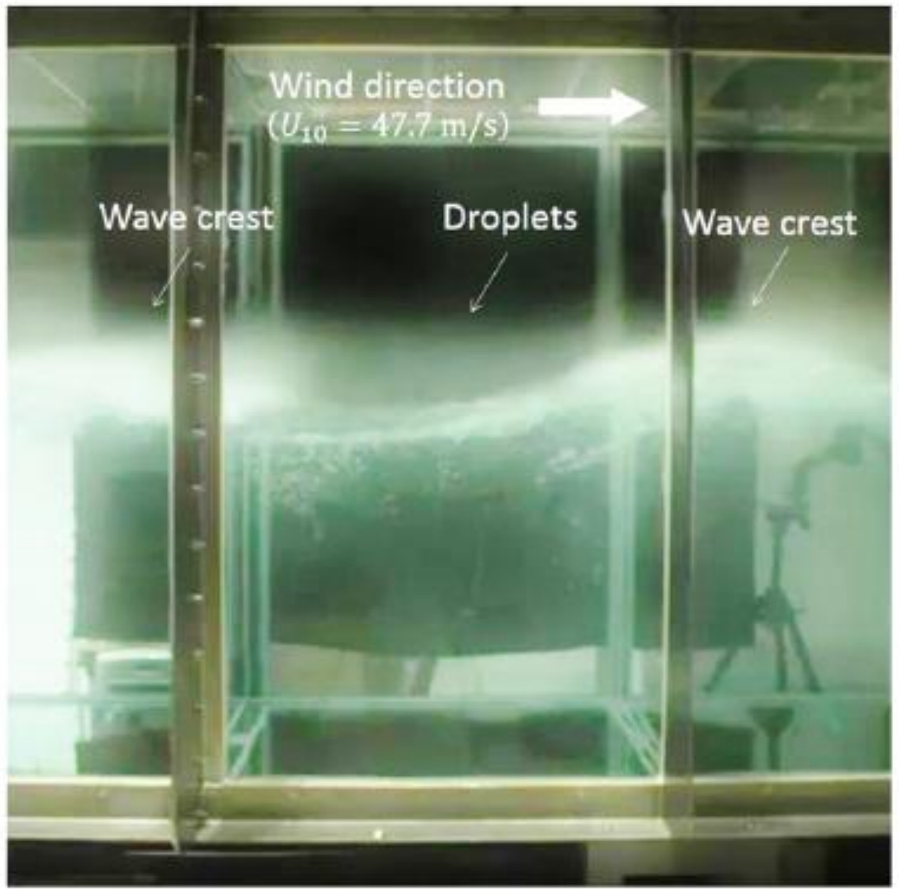

FIG. 6. Snapshot of droplets dispersing over breaking waves at $U_{10} = 47.7\,\mathrm{m\,s^{-1}}$.

Typical high-speed video image showing spray droplets shed by a breaking wave.

(Fairall et al.,2009)

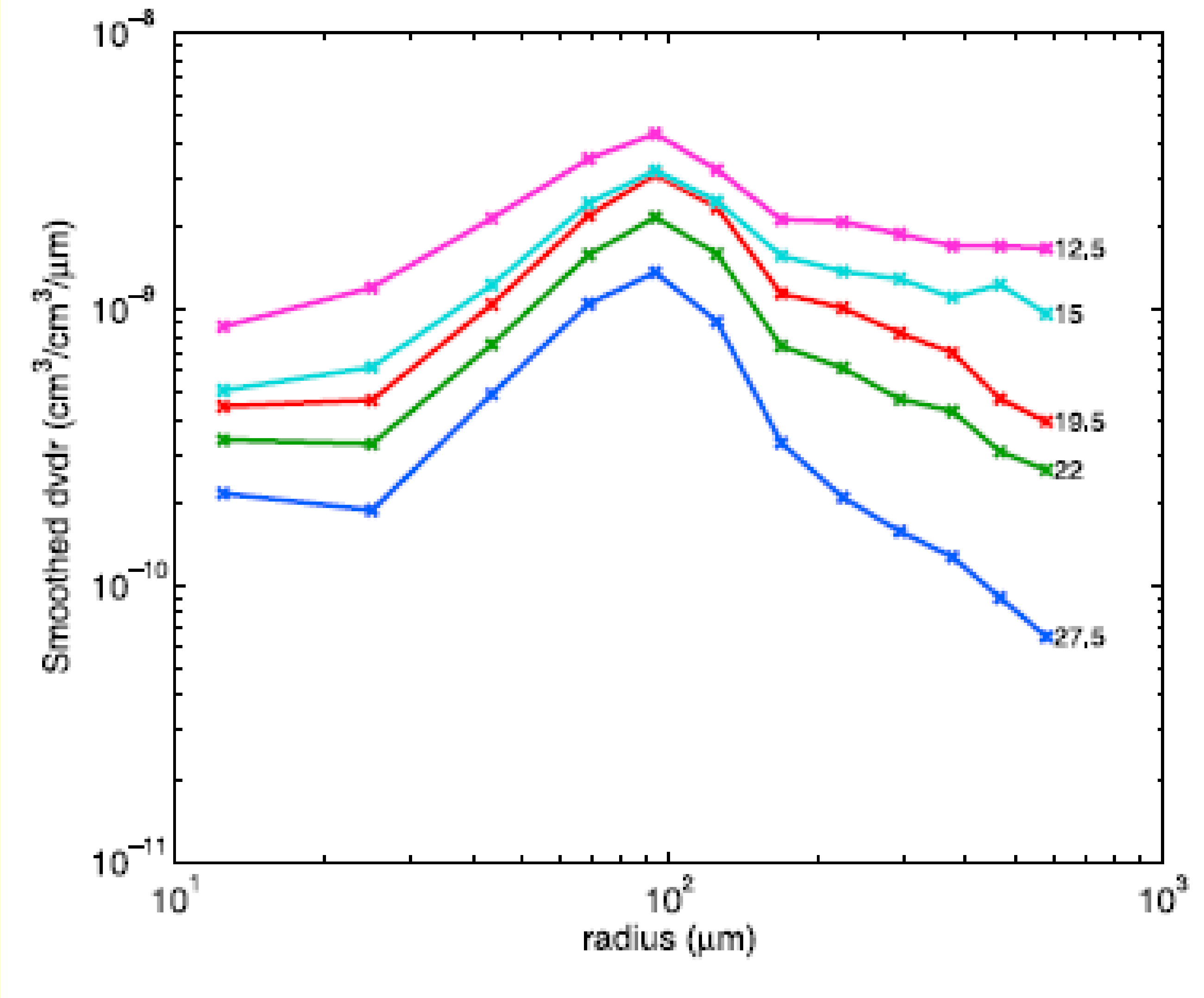

Droplet volume concentration for wind speed 16m/s at different heights above the water surface (in cm)

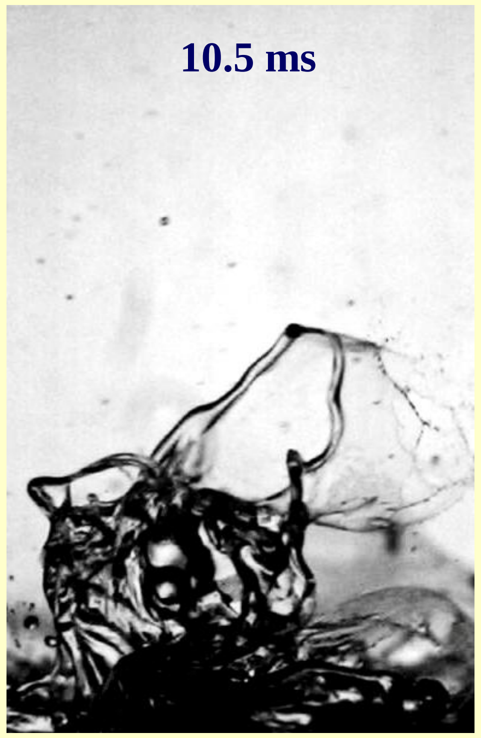

IAP RAS Lab experiment (Troitskayal et al.,2017)

Bag-break-up fragmentation mechanism is mainly responsible for spume-drops generation

Momentum, heat and moisture exchange between air and sea-spray drops

q – water vapor density
T_a, U_a - air temperature and velocity
T_w- water surface temperature
T_d, V_d droplet temperature and velocity
U_a – local air velocity

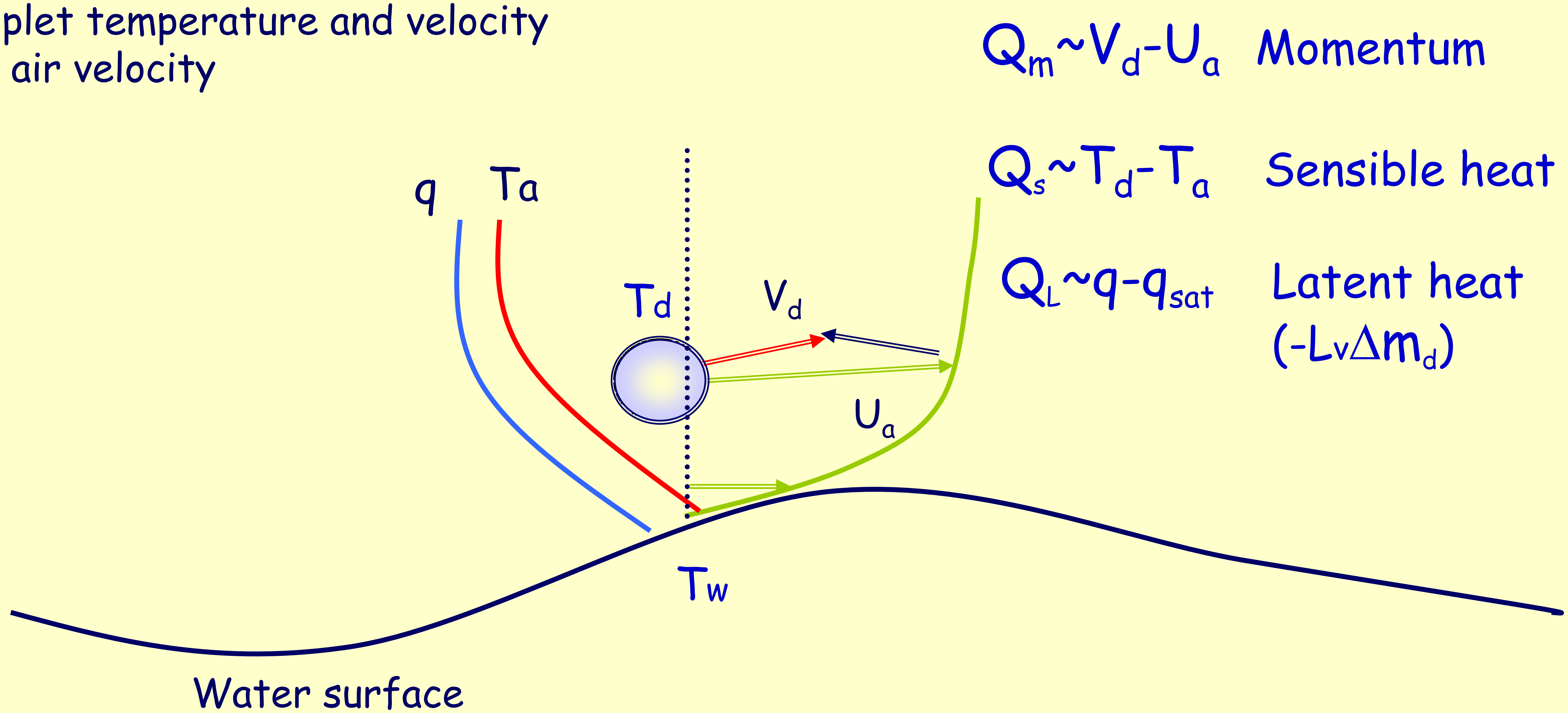

Filed experiment during typhoons “Skip” and “Tess” (USSR, 1988): cooling of the air boundary flow

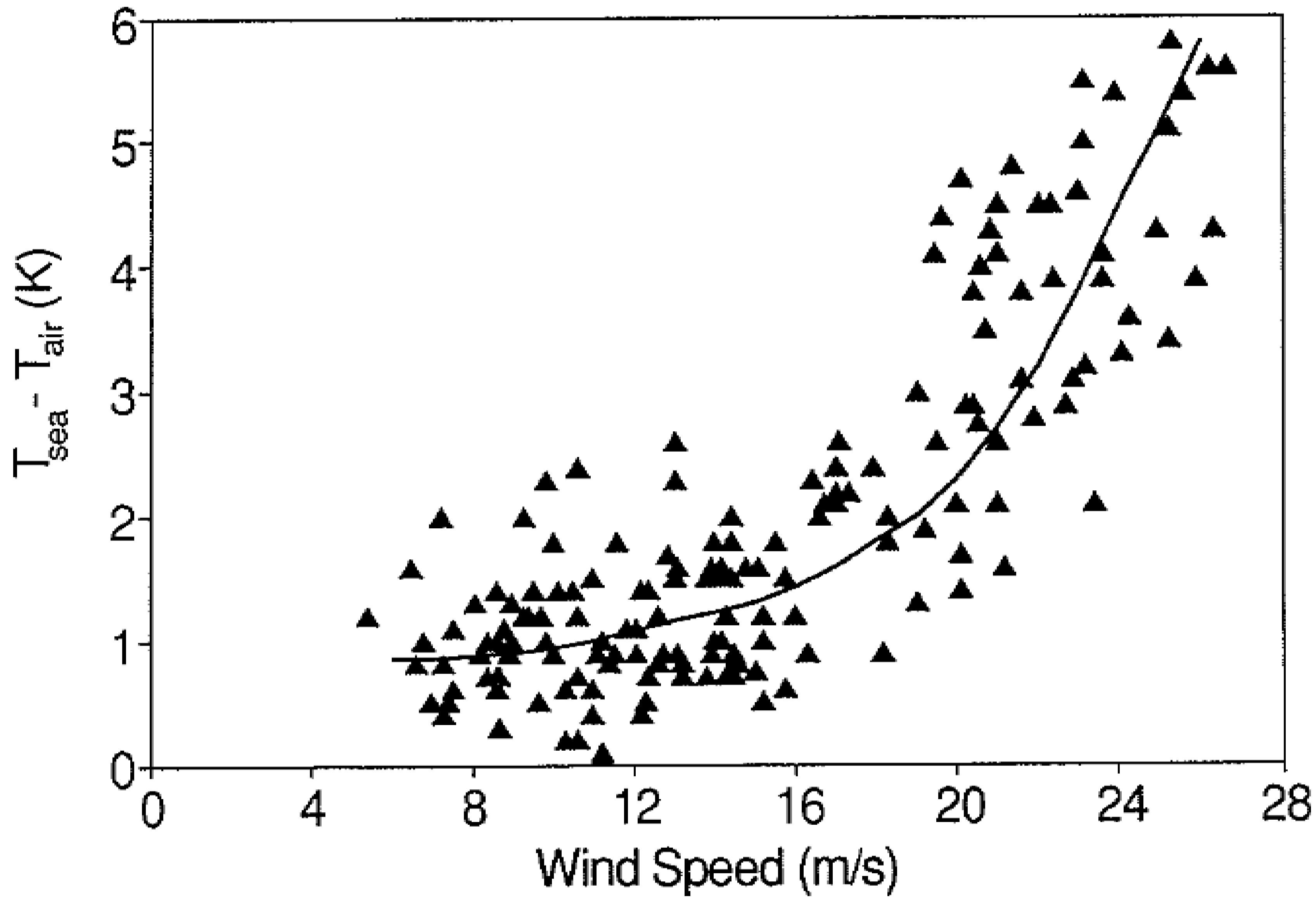

FIGURE 2 The marine boundary layer cooling associated with strong winds in two tropical cyclones, shown as a scatter diagram of observed air-sea temperature difference plotted against wind speed (Pudov, personal communication, 1991).

(From Fairall et al. 1994)

Phenomenological models

-Bulk algorithms (Fairall et al. 1994, Andreas et al. (2015): evaluate sensible and latent heat fluxes by summation of contributions of individual droplets by considering the differences between the initial and final droplets temperatures and sizes

-RANS models (Kudryavtsev & Makin 2011, Bianco et al. 2011): consider Reynolds –averaged (RANS) equations where the impact of drops on the air mometum, temperature and humidity is modeled by source functions obtained by closure assumptions.

Lagrangian stochastic models

Edson & Fairall (1994), Mueller & Veron (2014), Troitskaya et al. (2016): numerical simulation of the dynamics of individual drops in a prescribed mean air flow field and turbulent fluctuations of the surrounding air fields modeled by an artificial stochastic component.

Direct numerical simulation

Druzhinin et al. (2017,2018), Peng & Richter (2017, 2019): Solve primitive Navier-Stokes equations for a turbulent droplet-laden boundary-layer flow taking into account momentum and latent and sensible heat exchange between air and droplets.

Objective

To perform LES of a turbulent, droplet-laden air flow over waved water surface and investigate the influence of air and water surface temperatures on momentum, sensible and latent heat fluxes from droplets to air.

Two sets of boundary conditions for air and water temperatures are considered:

"Tropical Cyclone": $T_a = 27^oC$, $T_w = 28^oC$
"Polar Low": $T_a = -10^oC$, $T_w = 0^oC$

Humidity $H_a = 80\%$, $H_w = 98\%$

Schematic of numerical experiment

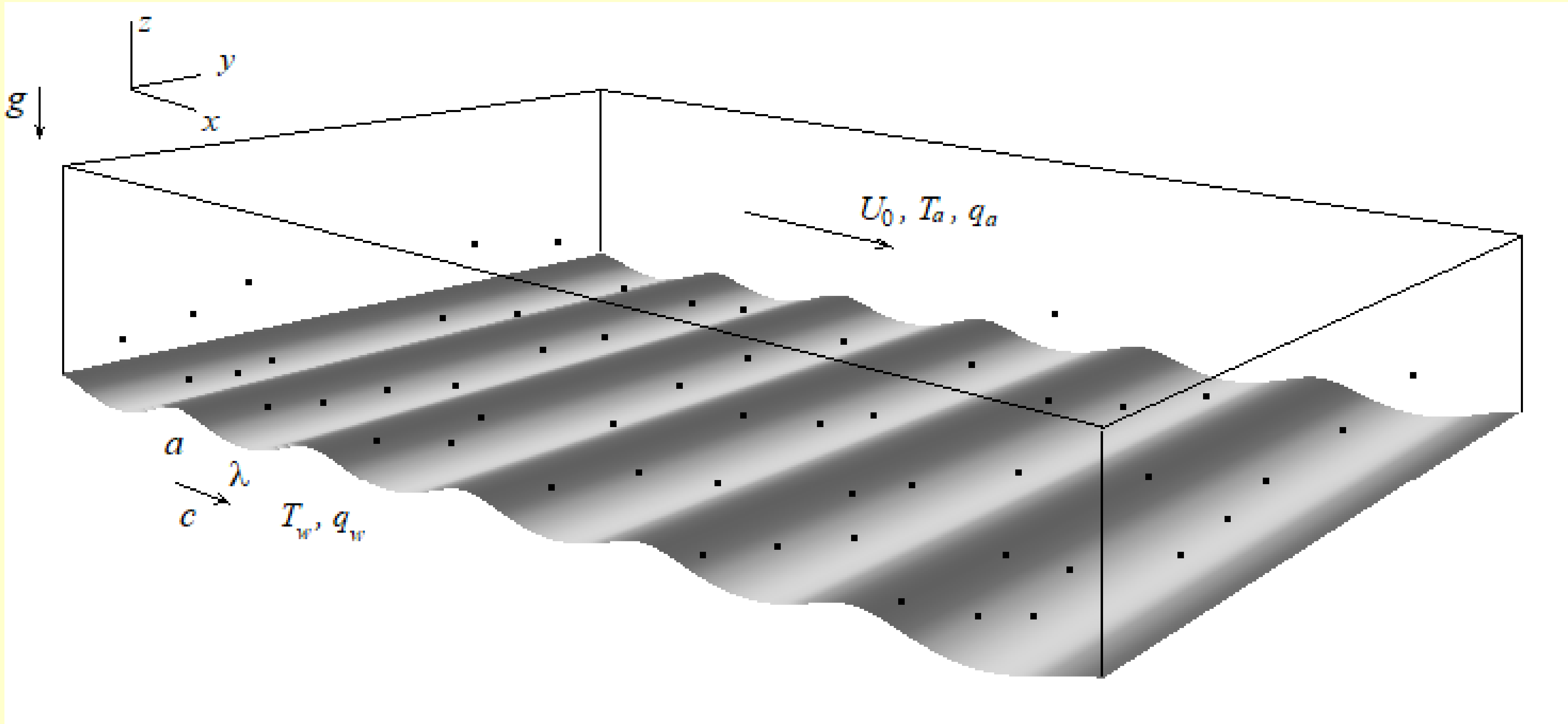

c=0.05 – wave celerity

ka =0.2 – maximum wave slope

Domain sizes: $L_x = 6\lambda \quad L_y = 4\lambda \quad L_z = \lambda$

$$\mathrm{Re} = \frac{U_0\lambda}{\nu} = 10^5$$ - bulk Reynolds number

CURVILINEAR COORDINATES

$$x = \xi - a\exp(-k\eta)\sin k\xi$$

$$z = \eta + a\exp(-k\eta)\cos k\xi$$

Shape of the water surface: $$z_b(x) = a\cos kx + \frac{1}{2}a^2k(\cos 2kx - 1)$$

Mapping over η: $$\eta = 0.5\left(1 + \frac{\tanh\tilde{\eta}}{\tanh 1.5}\right) \qquad -1.5 < \tilde{\eta} < 1.5$$

Grid of 360 x 240 x 180 nodes is employed

GOVERNING EQUATIONS: AIR FLOW
Eulerian framework

Momentum

$$\frac{\partial U_i}{\partial t}+\frac{\partial (U_i U_j)}{\partial x_j}=-\frac{\partial P}{\partial x_j}+\frac{1}{\mathrm{Re}}\frac{\partial^2 U_i}{\partial x_j \partial x_j}-\frac{\partial \tau_{ij}^U}{\partial x_j},$$

Continuity

$$\frac{\partial U_j}{\partial x_j}=0,$$

Temperature
Humidity

$$\frac{\partial (T,q)}{\partial t}+\frac{\partial [(T,q)U_j]}{\partial x_j}=\frac{1}{\mathrm{Pr}_{T,q}}\frac{\partial^2 (T,q)}{\partial x_j \partial x_j}-\frac{\partial \tau_j^{T,q}}{\partial x_j}$$

Subgrid closure
(Sullivan et al. 2008)

$$\tau_{ij}^U=-\nu_t\left(\frac{\partial U_i}{\partial x_j}+\frac{\partial U_j}{\partial x_i}\right),\quad \tau_j^{T,q}=-3\nu_t\frac{\partial (T,q)}{\partial x_j},$$

$$\nu_t=c_k e^{1/2} l,\quad l=\left(\Delta x_1 \Delta x_2 \Delta x_3\right)^{1/3}.$$

Subgrid TKE

$$\frac{\partial e}{\partial t}+\frac{\partial (U_j e)}{\partial x_j}=-\frac{\tau_{ij}^U}{2}\left(\frac{\partial U_i}{\partial x_j}+\frac{\partial U_j}{\partial x_i}\right)+2\frac{\partial}{\partial x_j}\left(\nu_t\frac{\partial e}{\partial x_j}\right)-c_D\frac{e^{3/2}}{l}.$$

Air velocity, temperature and humidity mean profiles

Velocity

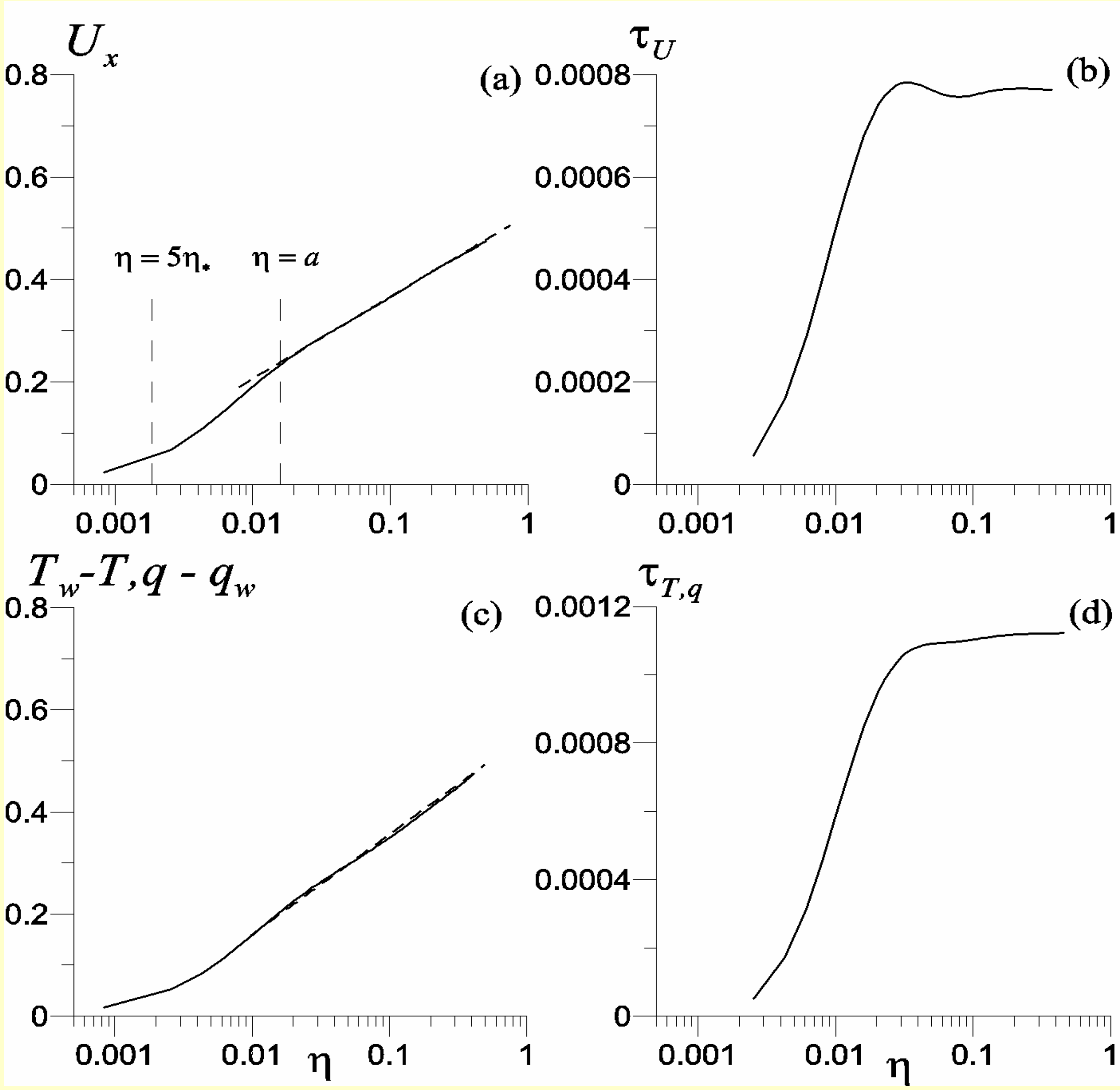

Temperature (Humidity)

$$u_* = \tau_U^{1/2}\Big|_{\eta=0.5}$$

$$T_* = \tau_T\Big|_{\eta=0.5} \Big/ u_*$$

$$q_* = \tau_q\Big|_{\eta=0.5} \Big/ u_*$$

Enthalpy sea-air flux

$$E_{int} = \rho_a c_a u_* T_* + L_v u_* q_*$$

----- $U = 2.5 u_* \ln\left(z / z_U\right)$ $\quad z_U = 0.11 z_* + 0.05a$

----- $T = 2.5 T_* \ln\left(z / z_T\right)$ $\quad z_{T,q} = z_U \left[2.67\left(u_* z_U \,\mathrm{Re}\right)^{0.25} - 2.57\right]^{-1}$

----- $q = 2.5 q_* \ln\left(z / z_q\right)$

Predictions by Monin-Obukhov similarity theory with roughness scales by TOGA-COARE algorithm (Zeng, et al. 1998)

Droplets Lagrangian dynamics

Coordinate $$\frac{dr_i^n}{dt} = V_i^n,$$

Velocity $$\frac{dV_i^n}{dt} = \frac{1}{\tau_d^n}\left(U_i^n - V_i^n\right)\left(1 + 0.15\,\mathrm{Re}_n^{0.687}\right) - g'\delta_{iz},$$

$$\mathrm{Re}_n = \frac{|U(r^n) - V^n|\, d_n}{\nu}$$

droplet Reynolds number

Temperature $$m_n c_w \frac{dT_n}{dt} = -Q_S^n - Q_L^n,$$

$$\tau_d^n = \frac{d_n^2}{18\nu}\frac{U_0}{\lambda}\frac{\rho_n}{\rho_a}$$

droplet relaxation time

Mass $$\frac{dm_n}{dt} = -L_v^{-1} Q_L^n.$$

Droplet-to-air sensible heat flux

$$Q_S^n = 2\pi c_a \rho_a \kappa d_n \left(T_n - T\left(r^n\right)\right)\left(1 + 0.25\,\mathrm{Re}_n^{0.5}\right)$$

Droplet-to-air latent heat flux

$$Q_L^n = -L_v \frac{dm_n}{dt} = 2\pi D L_v d_n \left(\rho_{sat,n}^v - \rho_a q\left(r^n\right)\right)\left(1 + 0.25\,\mathrm{Re}_n^{0.5}\right)$$

Droplets trajectories

TC PL

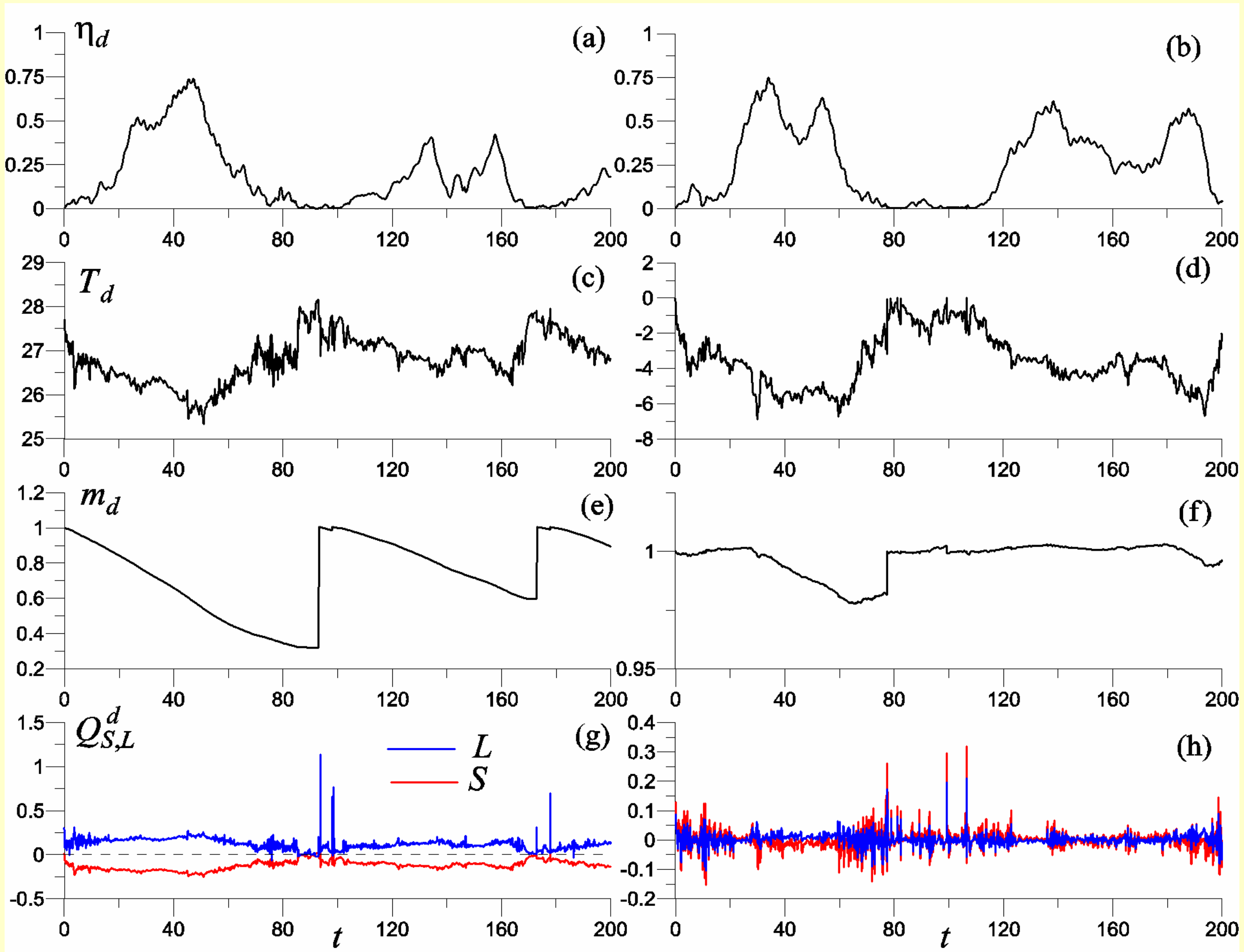

d=100 μm

TC PL

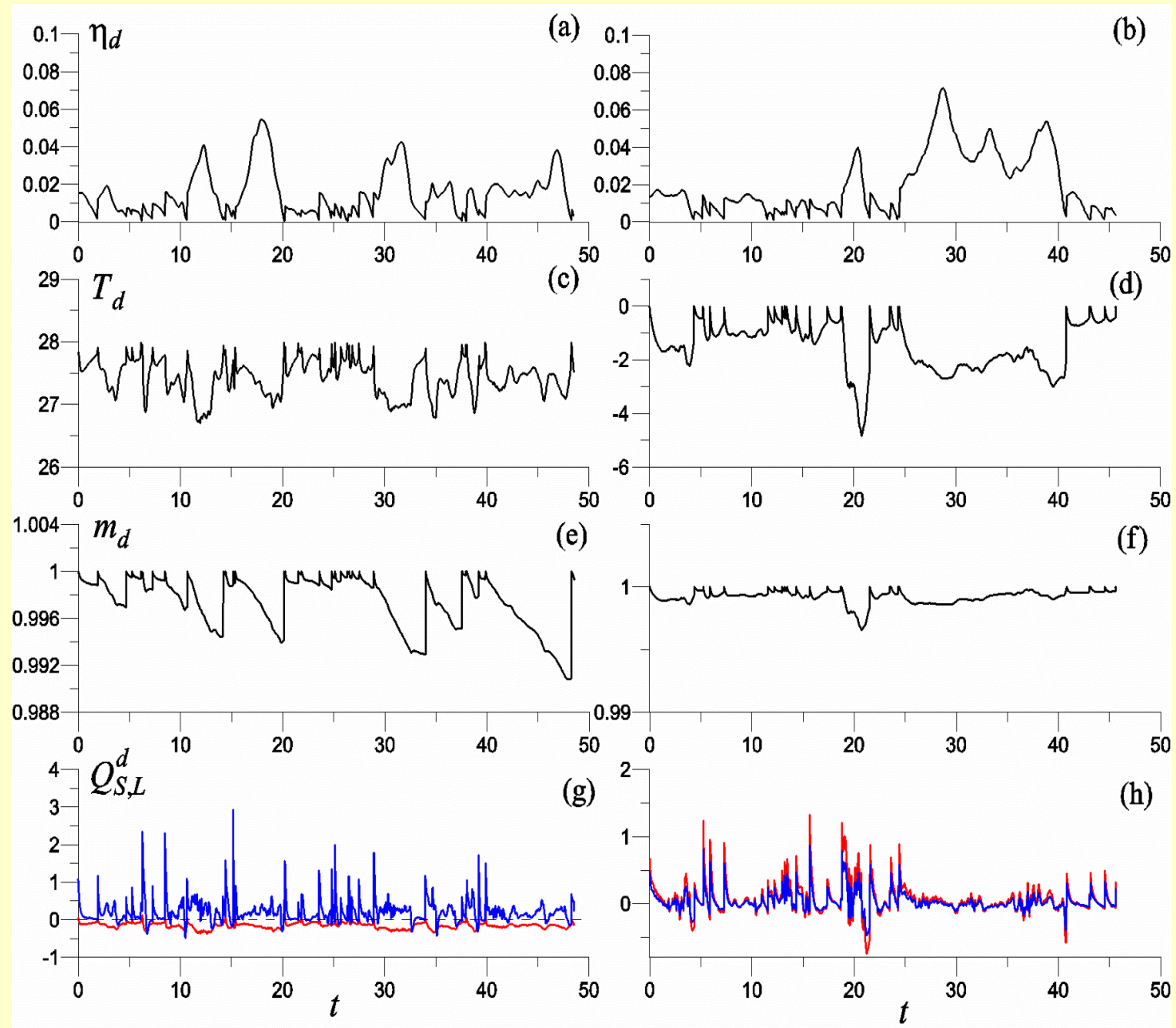

d=200 μm

$$Q_S^d + Q_L^d \approx 0$$

Heat fluxes

TC PL

$$E = Q_S + Q_L$$

$$E_{int} = \rho_a c_a u_* T_* + L_v u_* q_*$$

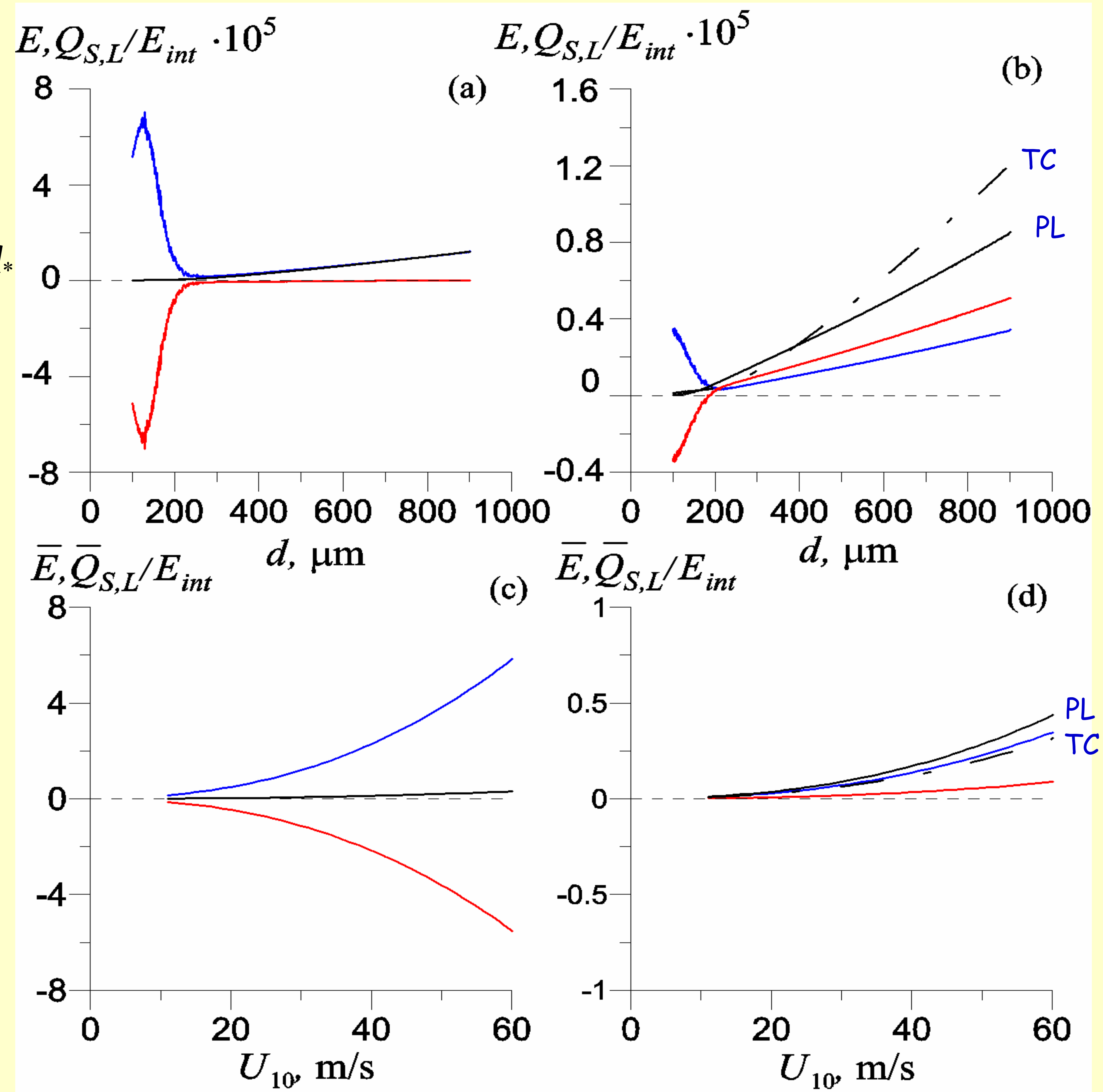

$Q_{S,L}$ – ensemble-averaged heat from a droplet to air during its "life" time

$$\bar{Q}_{S,L} = \int_{d=100\,\mu m}^{d=900\,\mu m} Q_{S,L} \frac{dF}{dr} dr$$

$\bar{Q}_{S,L}$ – mean heat flux from droplets to air for a given SGF

dF/dr –Spray Generation Function (Fairall 1994)

Заключение

Потоки явного и скрытого тепла от капель к воздуху, Q_S и Q_L, существенно зависят от балковых температур поверхности воды и воздуха:

- в условиях тропического циклона ($T_a=27^0C$, $T_w=28\ ^0C$) $Q_S<0$, $Q_L>0$ - мелкие капли охлаждают и увлажняют воздух, а ненулевой вклад в поток энтальпии дают лишь капли с размером более 200 μm за счет их испарения;

-в условиях полярного циклона ($T_a = -10^0C$, $T_w = 0^0C$) процесс испарения капель протекает существенно менее интенсивно, капли с размером более 200 μm дают ненулевой вклад в поток энтальпии и нагревают и увлажняют воздух.

В обоих случаях поток энтальпии $E=Q_S+Q_L$ положителен, и существенно возрастает с увеличением скорости ветра, до 30% и 50% при U > 50 m/s от турбулентного потока энтальпии погранслоя в условиях тропического и полярного циклонов.

Droplets "life" time

$t_d = (t_f - t_0)/N_{inj}$